

Article

# Intercomparison of Carbon Dioxide Products Retrieved from GOSAT Short-Wavelength Infrared Spectra for Three Years (2010–2012)

Anjian Deng <sup>1,2,3</sup>, Tao Yu <sup>1</sup>, Tianhai Cheng <sup>1,\*</sup>, Xingfa Gu <sup>1</sup>, Fengjie Zheng <sup>1</sup> and Hong Guo <sup>1</sup>

<sup>1</sup> Institute of Remote Sensing and Digital Earth, Chinese Academy of Sciences, 20A North Datun Road, Beijing 100101, China; anjie1030@126.com (A.D.); yutao@radi.ac.cn (T.Y.); guxf@radi.ac.cn (X.G.); zhengfj@radi.ac.cn (F.Z.); guohong@radi.ac.cn (H.G.)

<sup>2</sup> School of Surveying and Land Information Engineering, Henan Polytechnic University, 2001 Century Road, Jiaozuo 454000, China

<sup>3</sup> University of Chinese Academy of Sciences, 19A Yuquan Road, Beijing 100049, China

\* Correspondence: chength@radi.ac.cn; Tel.: +86-10-6483-9949

Academic Editor: Robert W. Talbot

Received: 28 July 2016; Accepted: 18 August 2016; Published: 23 August 2016

**Abstract:** This paper presents the comparison of two CO<sub>2</sub> datasets from the National Institute for Environmental Studies (NIES) of Japan and the Atmospheric CO<sub>2</sub> Observations from Space (ACOS) of NASA for three years (2010 to 2012). Both CO<sub>2</sub> datasets are retrieved from the Greenhouse gases Observing SATellite (GOSAT) short-wavelength infrared spectra over High gain surface land. In this three-year period, the yield of the NIES CO<sub>2</sub> column averaged dry air mole fractions (XCO<sub>2</sub>) is about 71% of ACOS retrievals. The overall bias is  $0.21 \pm 1.85$  ppm and  $-0.69 \pm 2.13$  ppm for ACOS and NIES XCO<sub>2</sub>, respectively, when compared with ground-based Fourier Transform Spectrometer (FTS) observations from twelve Total Carbon Column Observing Network (TCCON) sites. The differences in XCO<sub>2</sub> three-year means and seasonal means are within about 1 to 2 ppm. Strong consistency is obtained for the ACOS and NIES XCO<sub>2</sub> monthly averages time series over different regions, with the greatest mean difference of ACOS to NIES monthly means over China ( $1.43 \pm 0.60$  ppm) and the least over Brazil ( $-0.03 \pm 0.64$  ppm). The intercomparison between the two XCO<sub>2</sub> datasets indicates that the ACOS XCO<sub>2</sub> is globally higher than NIES by about 1 ppm and has smaller bias and better consistency than NIES data.

**Keywords:** atmospheric CO<sub>2</sub>; GOSAT; ACOS; comparison; difference

## 1. Introduction

Atmospheric carbon dioxide (CO<sub>2</sub>) is the most important greenhouse gas. The column averaged dry air mole fractions of atmospheric CO<sub>2</sub> (XCO<sub>2</sub>) has increased dramatically from 280 parts per million (ppm) in the pre-industrial era to 396 ppm in 2013 [1], most probably due to human activities, such as fossil fuel combusting, land use change, cement production and biomass burning. The resulting warming effect of increasing CO<sub>2</sub> concentration is predicted to lead to a rising surface temperature, rising sea levels and frequent occurrence of extreme weather conditions [2]. To reliably predict the impact of atmospheric CO<sub>2</sub> on global climate change, it is necessary to clarify the distribution and variation of atmospheric CO<sub>2</sub> concentration, as well as its source and sink.

Ground-based observations of greenhouse gas can provide accurate and high-frequent CO<sub>2</sub> measurements. However, their sparse and uneven global distributions lead to large uncertainties in the estimates of CO<sub>2</sub> amount and flux on sub-continental or regional spatial scales [3–5]. Theoretical studies show that satellite retrieval of atmospheric CO<sub>2</sub> has the potential to significantly reduce

the uncertainties in estimated CO<sub>2</sub> surface flux if the satellite observations are accurate and precise enough [6–9].

Greenhouse gases Observing SATellite (GOSAT) [10], launched in January 2009, was the world's first dedicated carbon satellite and has provided global multi-year observations with significant sensitivity near the surface. Based on the Short-Wavelength InfraRed (SWIR) spectra of GOSAT, two XCO<sub>2</sub> products were retrieved independently: the XCO<sub>2</sub> official product from the National Institute for Environmental Studies (NIES) of Japan [11–13] and the XCO<sub>2</sub> data product from Atmospheric CO<sub>2</sub> Observations from Space (ACOS) of NASA [14–16]. The research on the two products was extensive. Morino et al. [12] validated NIES GOSAT SWIR Level 2 v01.xx XCO<sub>2</sub> against the ground-based Fourier Transform Spectrometer (FTS) XCO<sub>2</sub> observations from the Total Carbon Column Observing Network (TCCON) and found that the NIES XCO<sub>2</sub> was biased by  $-8.85 \pm 4.75$  ppm. Yoshida et al. [13] presented that the NIES Level 2 v02.xx XCO<sub>2</sub> from an improved retrieval algorithm showed much smaller bias and standard deviation ( $-1.48$  and  $2.09$  ppm). Inoue et al. [17] compared NIES Level 2 v02.xx XCO<sub>2</sub> with aircraft-based data and the NIES XCO<sub>2</sub> was biased by  $-0.68 \pm 2.56$  ppm. Lei et al. [18] showed the comparison of NIES Level 2 v02.xx XCO<sub>2</sub> with model simulations and found that the XCO<sub>2</sub> was globally lower than the model by 2 ppm on average. For ACOS XCO<sub>2</sub>, Crisp et al. [16] reported the estimates of XCO<sub>2</sub> and analyzed the XCO<sub>2</sub> retrieval error characteristics. The preliminary validation of ACOS Level 2 v3.3 XCO<sub>2</sub> against TCCON data showed that the mean bias and standard deviation were 1.34 and 1.83 ppm [19]. Zhang et al. [20] examined the difference between ACOS Level 2 v3.3 XCO<sub>2</sub> and model simulations and found that the retrieved XCO<sub>2</sub> was higher than model by  $0.11 \pm 1.81$  ppm. Lindqvist et al. [21] evaluated the ACOS v3.5 XCO<sub>2</sub> seasonal cycle features with TCCON data. Kulawik et al. [22] validated the precision characteristics, season cycle, yearly growth and daily variability of ACOS v3.5 XCO<sub>2</sub> based on TCCON data.

These XCO<sub>2</sub> products were validated or compared with ground-based FTS data or model simulations. However, the validations or comparisons of the two XCO<sub>2</sub> products were carried out individually. The different characteristics between them remain unknown for different regions and times. Therefore, detailed analyses of the differences and suitabilities between the two XCO<sub>2</sub> products are essential for the evaluation of CO<sub>2</sub> retrieval algorithms and the combined applications of the two products, for example, combining the two products to generate improved datasets, and, in turn, to improve model prediction of global CO<sub>2</sub> source/sink. In this paper, we compare the NIES GOSAT SWIR Level 2 v02.xx XCO<sub>2</sub> (NIES XCO<sub>2</sub>) and ACOS GOSAT Level 2 v3.5 XCO<sub>2</sub> (ACOS XCO<sub>2</sub>) over land surfaces with High gain for the period of 2010 to 2012. We examine the difference of these two XCO<sub>2</sub> datasets to provide references for the evaluation of CO<sub>2</sub> retrieval algorithms and the suitability of the XCO<sub>2</sub> products in applications.

The paper is structured as follows. In Section 2, we describe the GOSAT and instruments, NIES and ACOS GOSAT XCO<sub>2</sub> products, and the main differences in ACOS and NIES XCO<sub>2</sub> retrieval algorithms. Section 3 presents the intercomparison and analysis between NIES and ACOS XCO<sub>2</sub> datasets for three years, and Section 4 provides the conclusions.

## 2. Data and Method

The analyzed time period spans three years, ranging from January 2010 to December 2012. The NIES GOSAT SWIR Level 2 v02.xx XCO<sub>2</sub> product and ACOS GOSAT Level 2 v3.5 XCO<sub>2</sub> retrievals are collected for the entire study period. As differences in the retrieval results still remain because of the High/Medium gain and land/ocean differences, the comparisons between NIES and ACOS XCO<sub>2</sub> are limited to High gain land surface in this work.

### 2.1. GOSAT and Instruments

GOSAT, which was launched on 23 January 2009, was the world's first satellite dedicated to measure the atmospheric CO<sub>2</sub> and methane (CH<sub>4</sub>). GOSAT was put in a sun-synchronous orbit at about 666 km with three-day recurrence. It was equipped with two instruments: Thermal and

Near infrared Sensor for carbon Observation-Fourier Transform Spectrometer (TANSO-FTS) and Cloud and Aerosol Imager (TANSO-CAI). TANSO-FTS is a Michelson interferometer and observes high-resolution spectra in three SWIR bands: 12,900 to 13,200  $\text{cm}^{-1}$  with 0.37  $\text{cm}^{-1}$  spectral resolution, 5800 to 6400  $\text{cm}^{-1}$  and 4800 to 5200  $\text{cm}^{-1}$  with 0.26  $\text{cm}^{-1}$  spectral resolution, and a TIR band: 700 to 1800  $\text{cm}^{-1}$  with 0.26  $\text{cm}^{-1}$  spectral resolution. The instantaneous field view of TANSO-FTS is about 15.8 mrad, corresponding to a nadir footprint diameter of about 10.5 km at sea level. The high spectral resolution spectra recorded by TANSO-FTS are analyzed to produce  $\text{CO}_2$  and  $\text{CH}_4$  products. TANSO-CAI is a radiometer used to detect optically thick clouds and aerosol inside the TANSO-FTS's field of view. For details on the GOSAT and the instruments, please refer to Kuze et al. [23].

## 2.2. NIES and ACOS GOSAT $\text{XCO}_2$ Products

The NIES GOSAT  $\text{XCO}_2$  data analyzed in this paper are the TANSO-FTS SWIR Level 2 v02.xx  $\text{XCO}_2$  product, which was produced by NIES of Japan. The NIES  $\text{XCO}_2$  product was retrieved from the absorption spectra within the three SWIR bands and represent  $\text{XCO}_2$  of a single measure point. All the column abundances of  $\text{CO}_2$  were successfully retrieved and passed the post-screening criteria [11–13]. After an improvement of the retrieval algorithm from v01.xx to 02.xx, the accuracy and precision of NIES GOSAT SWIR  $\text{XCO}_2$  has been improved significantly. The bias and standard deviation of NIES GOSAT v02.xx  $\text{XCO}_2$  were estimated to be about  $-1.48$  ppm and 2.09 ppm against the ground-based FTS  $\text{XCO}_2$  data from the TCCON sites [12,13].

After the loss of the Orbiting Carbon Observatory (OCO), the OCO science team was reformulated as the ACOS team by NASA and was invited to analyze the GOSAT data [15,16]. The ACOS GOSAT  $\text{XCO}_2$  used here was the Level 2 v3.5  $\text{XCO}_2$  retrieved from GOSAT TANSO-FTS SWIR Level 1B data. The ACOS  $\text{XCO}_2$  standard product contained all the soundings that converged in the retrieval [16,24]. According to the recommendations of ACOS Level 2 Standard Product Data User's Guide v3.5, the data screening and bias correction were applied to ACOS  $\text{XCO}_2$  before use [24].

## 2.3. The Main Differences between ACOS and NIES GOSAT $\text{XCO}_2$ Retrieval Algorithms

Although both ACOS and NIES GOSAT SWIR L2  $\text{XCO}_2$  retrieval algorithms are based on the optimal estimation methods [11,13,15,16,25–27], there are still some specific differences between them. The NIES v02.xx retrieval algorithm conducts strict cloud screening and simultaneously retrieves the vertical profile of four typical aerosol species [13]. While there was no similar sensor sensitive to clouds on OCO-2, the ACOS L2 v3.5 retrieval algorithm applied Oxygen-A band only clear-sky retrieval to screen optically thick clouds, and retrieved the profile of two aerosol types and two cloud types simultaneously [15,24]. These differences in the handling of light scattering may lead to different retrieval results. The  $\text{CO}_2$  absorption cross-sections around 2.06  $\mu\text{m}$  band were scaled by 0.99 to get more consistent results with the 1.61  $\mu\text{m}$  band in the ACOS retrieval algorithm [19]. This could cause large changes in the  $\text{XCO}_2$  retrieval results. There were still some differences in the pre-/post-processing between the two retrieval algorithms, such as the solar zenith angles requirements, and the aerosol optical depth (AOD) filtering [13,15,16,24]. These factors could affect the yields of the retrieval algorithm. In addition, to get high quality retrieval results, the ACOS  $\text{XCO}_2$  are screened using the updated screening criteria and underwent the bias correction to correct global bias and errors additionally according to the recommendations of ACOS [14,16,24]. This could further improve the consistency of the ACOS retrieval with respect to TCCON observations.

## 3. Results and Discussion

### 3.1. Comparisons with TCCON $\text{XCO}_2$

In order to quantitatively examine the differences between the ACOS and NIES  $\text{XCO}_2$ , the ACOS and NIES  $\text{XCO}_2$  datasets are compared with ground-based FTS  $\text{XCO}_2$  observations from twelve TCCON sites shown in Table 1. The ground-based FTS records high spectral resolution

( $0.02 \text{ cm}^{-1}$ ) direct solar spectra in the near infrared spectrum and the  $\text{CO}_2$  column concentrations are determined using the GGG software (GGG 2014, California Institute of Technology, California, CA, USA) based on the nonlinear least squares fitting. The uncertainty of the TCCON  $\text{XCO}_2$  is estimated to be about 0.2% [28,29]. The TCCON data used here are the GGG2014 releases. To get matched data between satellite retrieval and ground-based data, the ground-based FTS data are within  $\pm 30$  min of GOSAT overpass time and averaged. The satellite retrievals data are collected within a  $\pm 3$  degrees latitude/longitude box centered at each FTS site. The comparison results are listed in Table 1, and the bias and corresponding standard deviation of each site are shown in Figure 1.

**Table 1.** Summary of comparison of ACOS and NIES  $\text{XCO}_2$  versus TCCON observations. Shown are the coincided number  $n$  between satellite retrievals and TCCON data, the mean difference  $d$  (station bias) and standard deviation  $\text{std}$  of their difference, and the correlation coefficients  $r$ . The global offset, which is averaged  $d$ , the regional precision, which is averaged  $\text{std}$ , the relative accuracy, which is a standard deviation of  $d$ , and the mean correlation, which is averaged  $r$ , are also given at the bottom of the table.

Sites	ACOS—TCCON				NIES—TCCON			
	$n$	$d$ (ppm)	$\text{std}$ (ppm)	$r$	$n$	$d$ (ppm)	$\text{std}$ (ppm)	$r$
Sodankyla (67.37°N, 26.63°E)	50	1.54	1.47	0.91	45	−0.91	1.93	0.89
Bialystok (53.23°N, 23.02°E)	93	−0.06	1.57	0.88	23	−0.22	1.84	0.78
Bremen (53.10°N, 8.85°E)	44	0.55	1.84	0.82	7	−0.81	1.58	0.66
Karlsruhe (49.1°N, 8.44°E)	131	1.28	2.56	0.62	10	0.53	1.14	0.85
Orleans (47.97°N, 2.11°E)	203	0.03	1.95	0.75	32	−0.40	2.22	0.48
Garmisch(47.48°N,11.06°E)	212	1.07	2.18	0.75	22	1.09	2.44	0.74
Park Falls (45.94°N, 90.27°W)	239	0.22	2.08	0.84	130	0.46	1.94	0.85
Lamont (36.6°N, 97.49°W)	1170	−0.23	1.43	0.88	27	−1.49	1.52	0.87
JPL, Pasadena (34.2°N, 118.18°W)	267	−0.49	2.28	0.69	111	−2.35	2.47	0.68
Darwin (12.43°S, 130.89°E)	281	0.78	1.21	0.61	85	−0.59	1.29	0.36
Wollongong (34.41°S, 150.88°E)	508	0.56	1.91	0.63	36	−0.91	1.09	0.88
Lauder (45.04°S, 169.68°E)	126	0.34	1.62	0.77	70	−0.78	1.65	0.76
Global offset (ppm)			0.47				−0.53	
Regional precision (ppm)			1.84				1.76	
Relative accuracy (ppm)			0.62				0.93	
Mean correlation			0.76				0.73	

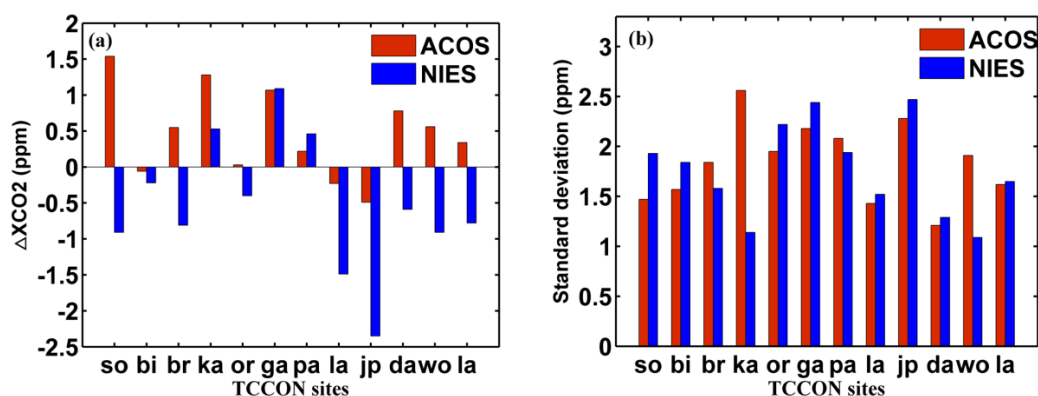


**Figure 1.** The column averaged dry air mole fractions of atmospheric carbon dioxide ( $\text{XCO}_2$ ) bias (a) and standard deviation (b) of the Atmospheric  $\text{CO}_2$  Observations from Space (ACOS) and the National Institute for Environmental Studies (NIES) versus Total Carbon Column Observing Network (TCCON) observations listed in Table 1. The TCCON sites are arranged from high to low latitude.

According to Table 1, both ACOS and NIES  $\text{XCO}_2$  are in good agreement with ground-based data from the correlation coefficients, with the mean correlation coefficients of ACOS and NIES with respect to TCCON 0.76 and 0.73, respectively. The station biases of ACOS  $\text{XCO}_2$  show most positive values

with the exception of Bialystok, Lamont and JPL Pasadena, while the NIES XCO<sub>2</sub> shows the mostly negative bias with the exception of Karlsruhe, Garmisch and Park Falls sites. In addition, according to Figure 1, the standard deviation of ACOS is slightly larger than that of NIES for most sites.

Figure 2 shows the histograms of differences of ACOS relative to TCCON and NIES relative to TCCON for all TCCON sites. The overall bias for ACOS and NIES are 0.21 and  $-0.69$  ppm, respectively. The standard deviation of XCO<sub>2</sub> differences for ACOS (1.85 ppm) is slightly smaller than NIES (2.13 ppm), indicating better consistency and less potential outliers. The relative accuracy, which indicates the relative regional-scale accuracy, is another important error estimate. The relative accuracy is 0.62 ppm for ACOS and 0.93 ppm for NIES dataset, as reported in Table 1. Through comparison with TCCON XCO<sub>2</sub>, the ACOS dataset is globally higher than NIES by about 1 ppm on average. In addition, the ACOS has smaller bias and standard deviation than NIES. Since the ACOS retrievals underwent recommended bias correction where the bias-correcting variables and coefficients were derived from TCCON and model data [14,16,24], the agreement between ACOS and TCCON data was improved substantially.

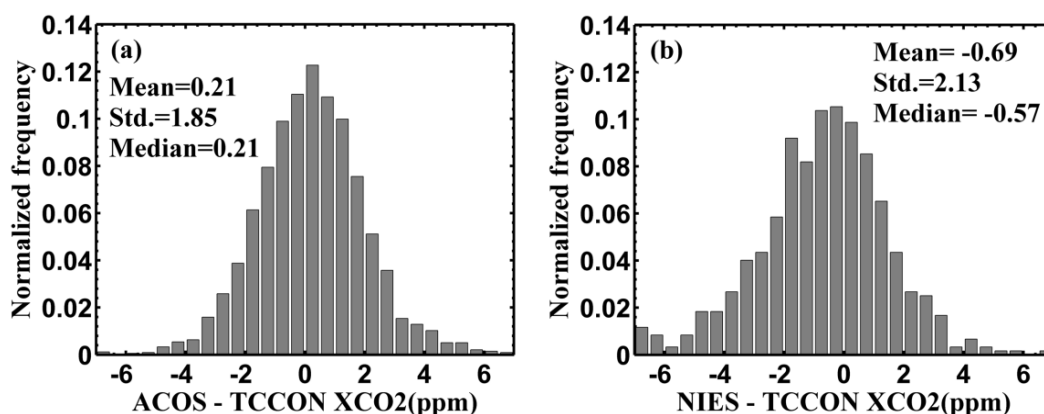


**Figure 2.** Histogram of the difference of ACOS relative to TCCON (a) and NIES relative to TCCON (b) for all TCCON sites listed in Table 1.

### 3.2. Comparisons of XCO<sub>2</sub> Yields and Three-Year Averages

As seen in Table 1, the number of ACOS retrievals matched with TCCON data is significantly more than NIES. In order to compare the yields of ACOS and NIES XCO<sub>2</sub> retrievals, Figure 3 presents the monthly numbers of global ACOS and NIES dataset over High gain land surface. Both ACOS and NIES XCO<sub>2</sub> datasets plotted in Figure 3 passed the post-screening filters. According to Figure 3, the yield of NIES XCO<sub>2</sub> is averagely 71% of that of ACOS retrievals, with the monthly number rates of NIES to ACOS ranging from 56% to 91%. Multiple factors contribute to the different yields. The NIES retrievals are limited to satellite scenes with solar zenith angles less than 70 degrees, which is less than that of ACOS (85 degrees) [11,16] and eliminates more NIES soundings in the pre-processing. The strategy and methods for cloud screening in ACOS retrievals differ from NIES and could also lead to different yields [11,13,16]. The more rigorous aerosol optical depth (AOD) filter in the NIES post-screening also rejects more retrievals than ACOS [13,16,24]. The number of XCO<sub>2</sub> retrievals showing a large seasonal variation also can be seen in Figure 3. This is because the GOSAT soundings with large solar zenith angles in northern high latitudinal regions in winter and early spring are filtered out. The snow-/ice-covered measurements are also removed by the blended albedo filter [13]. Furthermore, the content of desert dust and Asia aerosol is larger in Northern Hemisphere winter and spring and the GOSAT retrievals with high AOD are filtered out [13]. This seasonal characteristic of the desert dust and Asia aerosol could also contribute to the seasonal variations.

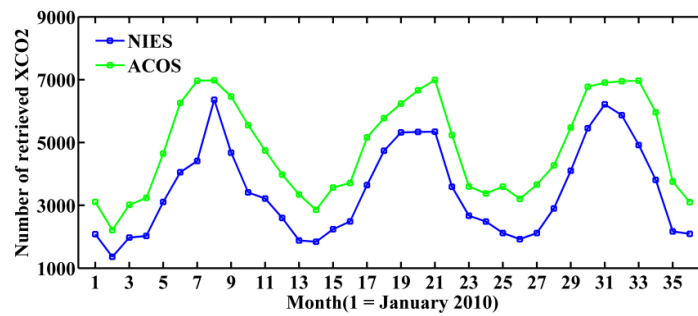


**Figure 3.** The monthly number time series of global retrieved NIES and ACOS XCO<sub>2</sub> passing the post-screening filters. The data is limited to High gain land surface.

Figure 4 shows the three-year average of ACOS and NIES XCO<sub>2</sub> and their differences (ACOS–NIES) from 2010 to 2012. The XCO<sub>2</sub> means are averaged only when there are more than three XCO<sub>2</sub> retrievals in each 2.5° × 2.5° latitude/longitude bin. As can be seen, the distribution of XCO<sub>2</sub> three-year averages of ACOS and NIES are very similar, with the correlation coefficient between the three-year averages of ACOS and NIES  $r = 0.73$ . The highest values are mainly located in East Asia, Central Africa, Northeast North American, and Central South America from both ACOS and NIES averages, indicating intense human activity and large carbon emissions over these regions. Moreover, about 80.3% of ACOS XCO<sub>2</sub> means are greater than NIES data as reported in Figure 4c. The mean difference between ACOS and NIES means is about 1.24 ppm with the standard deviation of 1.69 ppm as reported in Figure 4d.

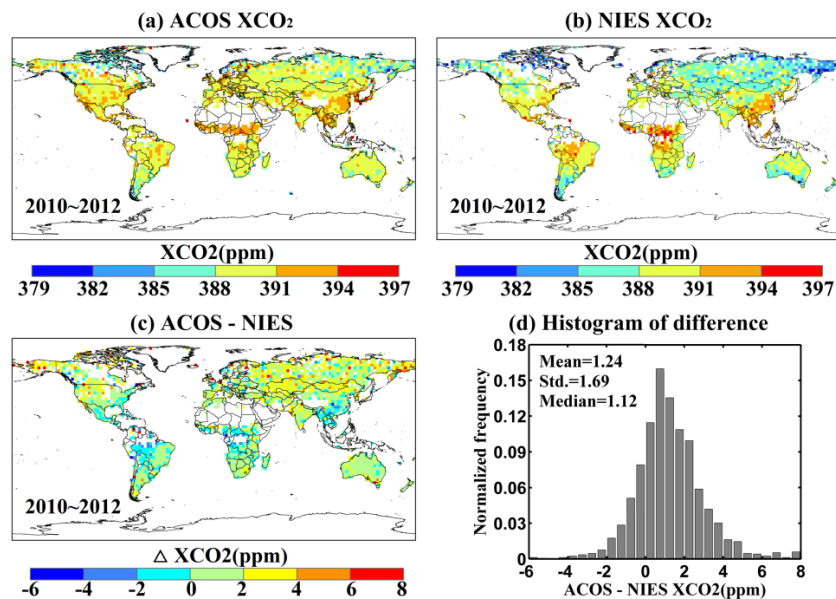


**Figure 4.** Global distribution of three-year averages of ACOS (a) and NIES (b) XCO<sub>2</sub> and their difference (c) gridded in 2.5° × 2.5° bins from 2010 to 2012; the histogram of difference shown in (c) is presented in (d).

### 3.3. Seasonal Difference between ACOS and NIES XCO<sub>2</sub>

To analyze the seasonal difference of XCO<sub>2</sub> retrievals, the seasonal means of NIES and ACOS GOSAT XCO<sub>2</sub> from December 2011 to November 2012 are selected and compared. The twelve months are grouped into four seasons: winter (December, January and February), spring (March, April and May), summer (June, July and August), and autumn (September, October and November). The corresponding XCO<sub>2</sub> seasonal means differences and the histograms of differences are shown in

Figure 5. As reported in Figure 5a, more than 80% of the ACOS XCO<sub>2</sub> means are greater than NIES for each season. The mean difference between ACOS and NIES XCO<sub>2</sub> seasonal means are about 1 ppm with a standard deviation in the range of 1 to 2 ppm. The greatest mean difference of XCO<sub>2</sub> occurs in summer and the smallest in winter.

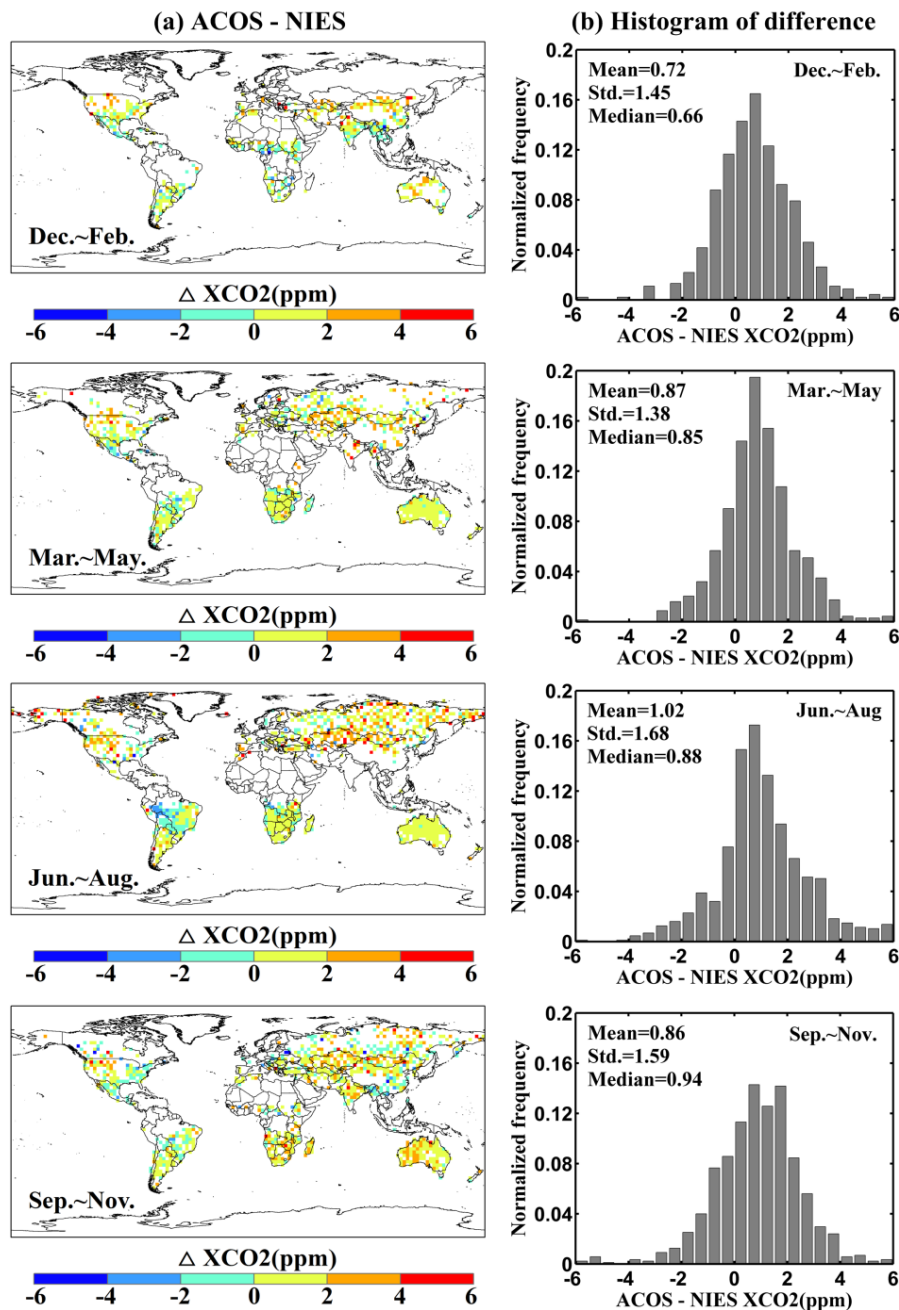
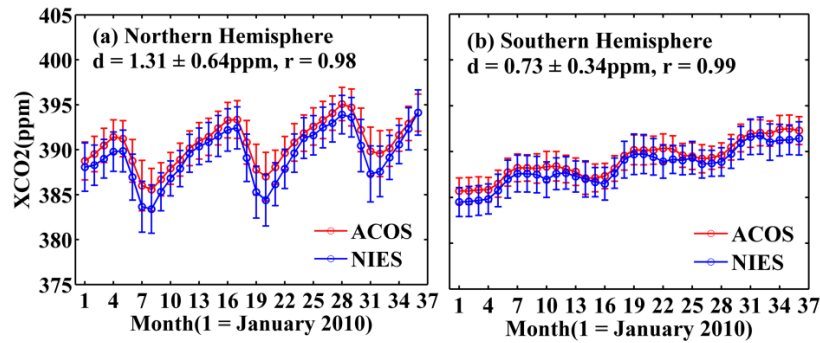


Figure 5. Seasonal difference (a) gridded in  $2.5^{\circ} \times 2.5^{\circ}$  bins between ACOS and NIES XCO<sub>2</sub> means and the histogram of their difference (b) in each season from December 2011 to November 2012.

### 3.4. Comparison between ACOS and NIES XCO<sub>2</sub> for Different Regions

Figure 6 shows the time series of XCO<sub>2</sub> monthly means over Northern and Southern Hemisphere during the three years. Overall, good agreement is obtained for the monthly averages of NIES and ACOS XCO<sub>2</sub> with respect to the amplitude and phase of XCO<sub>2</sub> seasonal cycle. Compared with the Southern Hemisphere, the mean difference d of XCO<sub>2</sub> monthly means over Northern Hemisphere

is slightly larger ( $1.31 \pm 0.64$  ppm compared with  $0.73 \pm 0.34$  ppm). In addition, the XCO<sub>2</sub> seasonal fluctuation over Northern Hemisphere is significantly higher than Southern Hemisphere from both NIES and ACOS XCO<sub>2</sub> monthly means. This is mainly because there is more land surface and the source/sink of CO<sub>2</sub> is more obvious in Northern Hemisphere [30].



**Figure 6.** Time series of NIES and ACOS XCO<sub>2</sub> monthly mean in the Northern (a) and Southern (b) Hemispheres for three years. The mean difference  $d$  of ACOS to NIES and its corresponding standard deviation, and the correlation coefficient  $r$  between NIES and ACOS are evaluated based on the XCO<sub>2</sub> monthly means.

To further examine the difference between ACOS and NIES XCO<sub>2</sub> for different regions, Figure 7 presents the XCO<sub>2</sub> monthly means over six typical countries or regions. As can be seen from Figure 7, the differences of XCO<sub>2</sub> monthly mean vary depending on the locations and months. Among the four northern countries or regions, the mean difference of XCO<sub>2</sub> monthly means is smallest over Europe ( $0.65 \pm 0.69$  ppm) and the largest over China ( $1.43 \pm 0.60$  ppm). As there are large amounts of human activity and complex CO<sub>2</sub> sources/sinks in China region, it may indicate large errors in the retrieval results for China region. In addition, the interference of high content and complex type of aerosol particles over China may also contribute to the difference between ACOS and NIES XCO<sub>2</sub> retrievals. The mean difference is slightly larger for the USA ( $1.27 \pm 0.47$  ppm) than Russia ( $1.05 \pm 0.57$  ppm). In the Southern Hemisphere, the XCO<sub>2</sub> monthly mean difference over Australia ( $1.17 \pm 0.37$  ppm) is significantly greater than that of Brazil ( $-0.03 \pm 0.64$  ppm).

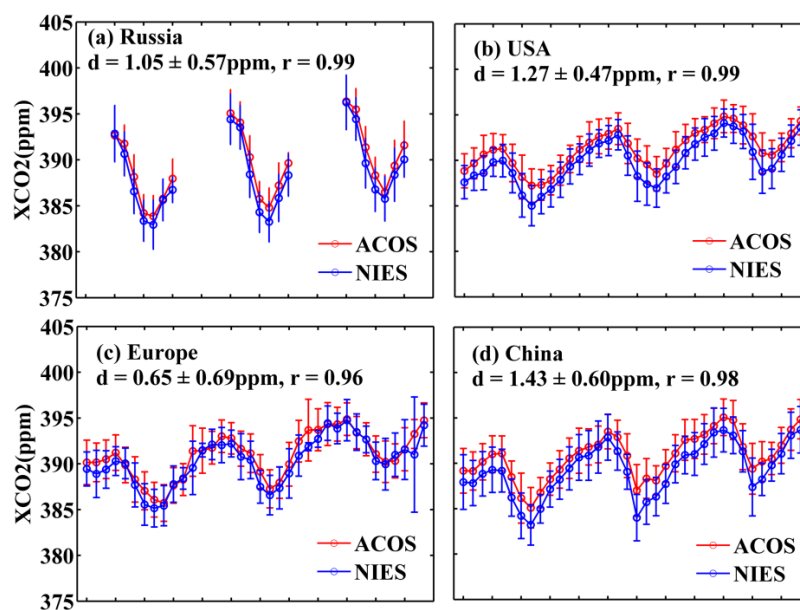


**Figure 7.** Cont.

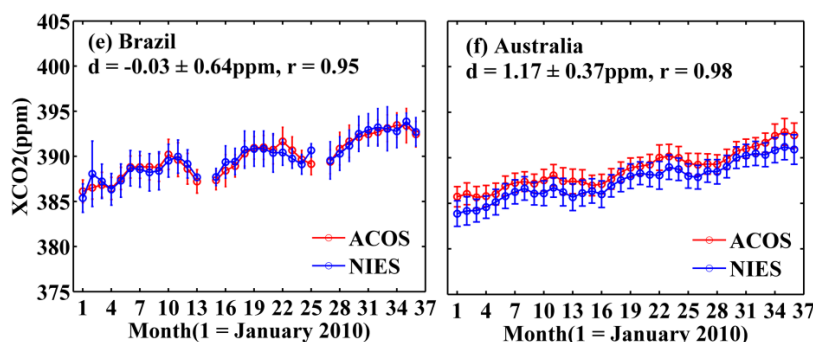


**Figure 7.** The same as Figure 6 but for six countries or regions. There are some XCO<sub>2</sub> monthly means unavailable over Russia and Brazil.

#### 4. Conclusions

The differences of ACOS and NIES GOSAT SWIR XCO<sub>2</sub> datasets over High gain land surface for three years (2010–2012) were investigated in this paper. Since both NIES and ACOS XCO<sub>2</sub> retrieval algorithms ingested GOSAT SWIR spectra and were based on the optimal estimation methods, good agreement was obtained for the CO<sub>2</sub> global distribution, seasonal variation and monthly average time series between them. However, discrepancies still existed in the two XCO<sub>2</sub> datasets. The yield of NIES XCO<sub>2</sub> was about 71% of ACOS retrievals passing the recommended post-retrieval screening criteria. This was mainly ascribed to difference in the aerosol optical depth (AOD) filtering criteria and the solar zenith degree requirement between the two retrieval algorithms.

The overall XCO<sub>2</sub> bias was  $0.21 \pm 1.85$  ppm and  $-0.69 \pm 2.13$  ppm for ACOS and NIES, respectively, when compared with TCCON observations. The relative regional-scale accuracy was 0.62 and 0.93 ppm for ACOS and NIES. The ACOS XCO<sub>2</sub> three-year means and seasonal means were generally greater than NIES by about 1 to 2 ppm. In addition, the mean differences between ACOS and NIES XCO<sub>2</sub> monthly means varied over different regions with the largest difference over China ( $1.43 \pm 0.60$  ppm) and the least over Brazil ( $-0.03 \pm 0.64$  ppm). The differences in the handling of light scattering in the retrieval algorithms may lead to the difference in retrieval results. Furthermore, the bias correction applied to the ACOS XCO<sub>2</sub> retrievals essentially reduced the global bias and enhanced the consistency with respect to TCCON data. The intercomparison between the two datasets indicates that ACOS XCO<sub>2</sub> is globally higher than NIES by about 1 ppm and has a smaller bias and better consistency than NIES datasets.

This paper provides a reference for the evaluation of NIES and ACOS XCO<sub>2</sub> retrieval algorithms and the suitability of the XCO<sub>2</sub> products in applications. As can be seen, the ACOS XCO<sub>2</sub> is generally higher than NIES retrievals. The difference between these two datasets is significantly large over the China region. It is suggested to further examine the difference of the two products from the aspects of approaches for retrieving cloud and aerosol optical properties, absorption spectroscopy of CO<sub>2</sub> and oxygen (O<sub>2</sub>), as well as instrument characteristics.

**Acknowledgments:** This research was supported by the Major Special Project of the China High-Resolution Earth Observation System (NO: Y4D00100GF; 30-Y20A21-9003-15/17), Natural Science Foundation of China (No: 41371015, 41501401, and 41001207), and Youth Innovation Promotion Association of CAS (No: 2011062). We kindly thank the GOSAT team for providing the NIES GOSAT Level 2 data product. We also thank the ACOS/OCO-2 project for the ACOS Level 2 version 3.5 XCO<sub>2</sub> product. TCCON data were obtained from the TCCON Data Archive, hosted by the Carbon Dioxide Information Analysis Center (CDIAC).

**Author Contributions:** Anjian Deng and Tianhai Cheng conceived and designed the experiments; Anjian Deng performed the experiments; Tianhai Cheng, Tao Yu, Xingfa Gu analyzed the data; Fengjie Zheng and Hong Guo helped perform the statistical analysis. Anjian Deng wrote the paper.

**Conflicts of Interest:** The authors declare no conflict of interest.

## References

1. World Data Centre for Greenhouse Gases. Available online: <http://ds.data.jma.go.jp/gmd/wdcgg/pub/global/globalmean.html> (accessed on 19 August 2016).
2. Solomon, S.; Qin, D.; Manning, M.; Chen, Z.; Marquis, M.; Averyt, K.B.; Tignor, M.; Miller, H.L. *Climate Change 2007: The Physical Science Basis, Contribution of Working Group 1 to the Fourth Assessment Report of the Intergovernmental Panel on Climate Change (IPCC)*; Cambridge University Press: Cambridge, UK, 2007.
3. Gurney, K.R.; Law, R.M.; Denning, A.S.; Rayner, P.J.; Baker, D.; Bousquet, P.; Bruhwiler, L.; Chen, Y.-H.; Ciais, P.; Fan, S. Towards robust regional estimates of CO<sub>2</sub> sources and sinks using atmospheric transport models. *Nature* **2002**, *415*, 626–629. [[CrossRef](#)] [[PubMed](#)]
4. Stephens, B.B.; Gurney, K.R.; Tans, P.P.; Sweeney, C.; Peters, W.; Bruhwiler, L.; Ciais, P.; Ramonet, M.; Bousquet, P.; Nakazawa, T.; et al. Weak northern and strong tropical land carbon uptake from vertical profiles of atmospheric CO<sub>2</sub>. *Science* **2007**, *316*, 1732–1735. [[CrossRef](#)] [[PubMed](#)]
5. Hungershoefer, K.; Breon, F.-M.; Peylin, P.; Chevallier, F.; Rayner, P.; Klonecki, A.; Houweling, S.; Marshall, J. Evaluation of various observing systems for the global monitoring of CO<sub>2</sub> surface fluxes. *Atmos. Chem. Phys.* **2010**, *10*, 503–520. [[CrossRef](#)]
6. Rayner, P.J.; O'Brien, D.M. The utility of remotely sensed CO<sub>2</sub> concentration data in surface source inversions. *Geophys. Res. Lett.* **2001**, *28*, 175–178. [[CrossRef](#)]
7. Houweling, S.; Breon, F.M.; Aben, I.; Rodenbeck, C.; Gloor, M.; Heimann, M.; Ciais, P. Inverse modeling of CO<sub>2</sub> sources and sinks using satellite data: A synthetic inter-comparison of measurement techniques and their performance as a function of space and time. *Atmos. Chem. Phys.* **2004**, *4*, 523–538. [[CrossRef](#)]
8. Miller, C.E.; Crisp, D.; DeCola, P.L.; Olsen, S.C.; Randerson, J.T.; Michalak, A.M.; Alkhaled, A.; Rayner, P. Precision requirements for space-based XCO<sub>2</sub> data. *J. Geophys. Res.* **2007**, *112*, D10314. [[CrossRef](#)]
9. Chevallier, F. Impact of correlated observation errors on inverted CO<sub>2</sub> surface fluxes from OCO measurement tents. *Geophys. Res. Lett.* **2007**, *34*, L24804. [[CrossRef](#)]
10. Yokota, T.; Yoshida, Y.; Eguchi, N.; Ota, Y.; Tanaka, T.; Watanabe, H.; Maksyutov, S. Global concentrations of CO<sub>2</sub> and CH<sub>4</sub> retrieved from GOSAT: First preliminary result. *Sola* **2009**, *5*, 160–163. [[CrossRef](#)]
11. Yoshida, Y.; Ota, Y.; Eguchi, N.; Kikuchi, N.; Nobuta, K.; Tran, H.; Morino, I.; Yokota, T. Retrieval algorithm for CO<sub>2</sub> and CH<sub>4</sub> column abundances from short-wavelength infrared spectral observations by the Greenhouse gases observing satellite. *Atmos. Meas. Tech.* **2011**, *4*, 717–734. [[CrossRef](#)]
12. Morino, I.; Uchino, O.; Inoue, M.; Yoshida, Y.; Yokota, T.; Wennberg, P.O.; Toon, G.C.; Wunch, D.; Roehl, C.M.; Notholt, J.; et al. Preliminary validation of column-averaged volume mixing ratios of carbon dioxide and methane retrieved from GOSAT short-wavelength infrared spectra. *Atmos. Meas. Tech.* **2011**, *4*, 1061–1076. [[CrossRef](#)]
13. Yoshida, Y.; Kikuchi, N.; Morino, I.; Uchino, O.; Oshchepkov, S.; Bril, A.; Saeki, T.; Schutgens, N.; Toon, G.C.; Wunch, D.; et al. Improvement of the retrieval algorithm for GOSAT SWIR XCO<sub>2</sub> and XCH<sub>4</sub> and their validation using TCCON data. *Atmos. Meas. Tech.* **2013**, *6*, 1533–1547. [[CrossRef](#)]
14. Wunch, D.; Wennberg, P.O.; Toon, G.C.; Connor, B.J.; Fisher, B.; Osterman, G.B.; Frankenberg, C.; Mandrake, L.; O'Dell, C.; Ahonen, P.; et al. A method for evaluating bias in global measurements of CO<sub>2</sub> total columns from space. *Atmos. Chem. Phys.* **2011**, *11*, 20899–20946. [[CrossRef](#)]
15. O'Dell, C.W.; Connor, B.; Boesch, H.; O'Brien, D.; Frankenberg, C.; Castano, R.; Christi, M.; Elderling, D.; Fisher, B.; Gunson, M.; et al. The ACOS retrieval algorithm—Part 1: Description and validation against synthetic observations. *Atmos. Meas. Tech.* **2012**, *5*, 99–121. [[CrossRef](#)]
16. Crisp, D.; Fisher, B.M.; O'Dell, C.; Frankenberg, C.; Basilio, R.; Boesch, H.; Brown, L.R.; Castano, R.; Connor, B.; Deutscher, N.M.; et al. The ACOS CO<sub>2</sub> retrieval algorithm—Part 2: Global XCO<sub>2</sub> data characterization. *Atmos. Meas. Tech.* **2012**, *5*, 687–707. [[CrossRef](#)]
17. Inoue, M.; Morino, I.; Uchino, O.; Miyamoto, Y.; Yoshida, Y.; Yokota, T.; Machida, T.; Sawa, Y.; Matsueda, H.; Sweeney, C.; et al. Validation of XCO<sub>2</sub> derived from SWIR spectra of GOSAT TANSO-FTS with aircraft measurement data. *Atmos. Chem. Phys.* **2013**, *13*, 9771–9788. [[CrossRef](#)]
18. Lei, L.P.; Guan, X.H.; Zeng, Z.C.; Zhang, B.; Ru, F.; Bu, R. A comparison of atmospheric CO<sub>2</sub> concentration GOSAT-based observations and model simulations. *Sci. China Earth Sci.* **2014**, *57*, 1393–1402. [[CrossRef](#)]

19. Goddard Earth Science Data Information and Services (GES DISC) of National Aeronautics and Space Administration (NASA). *ACOS Level 2 Standard Production Data User's Guide*; v3.3. National Aeronautics and Space Administration: Washington, DC, USA, 2013.
20. Zhang, H.F.; Chen, B.Z.; Xu, G.; Yan, J.W.; Che, M.L.; Chen, J.; Fang, S.F.; Lin, X.F.; Sun, S.B. Comparing simulated atmospheric carbon dioxide concentration with GOSAT retrievals. *Chin. Sci. Bull.* **2015**, *60*, 380–386. [[CrossRef](#)]
21. Lindqvist, H.; O'Dell, C.W.; Basu, S.; Boesch, H.; Chevallier, F.; Deutscher, N.; Feng, L.; Fisher, B.; Hase, F.; Inoue, M.; et al. Does GOSAT capture the true seasonal cycle of carbon dioxide? *Atmos. Chem. Phys.* **2015**, *15*, 13023–13040. [[CrossRef](#)]
22. Kulawik, S.; Wunch, D.; O'Dell, C.; Frankenberg, C.; Reuter, M.; Oda, T.; Chevallier, F.; Sherlock, V.; Buchwitz, M.; Osterman, G.; et al. Consistent evaluation of ACOS-GOSAT, BESD-SCIAMACHY, CarbonTracker, and MACC through comparisons to TCCON. *Atmos. Meas. Tech.* **2016**, *9*, 683–709. [[CrossRef](#)]
23. Kuze, A.; Suto, H.; Nakajima, M.; Hamazaki, T. Thermal and near infrared sensor for carbon observation Fourier-transform spectrometer on greenhouse gases observing satellite for greenhouse gases monitoring. *Appl. Opt.* **2009**, *48*, 6716–6733. [[CrossRef](#)] [[PubMed](#)]
24. Goddard Earth Science Data Information and Services (GES DISC) of National Aeronautics and Space Administration (NASA). *ACOS Level 2 Standard Production Data User's Guide*; v3.5. National Aeronautics and Space Administration: Washington, DC, USA, 2016.
25. Rodgers, C.D. *Inverse Methods for Atmospheric Sounding: Theory and Practice*; World Scientific: Singapore, 2000.
26. Boesch, H.; Toon, G.C.; Sen, B.; Washenfelder, R.A.; Wennberg, P.O.; Buchwitz, M.; de Beek, R.; Burrows, J.P.; Crisp, D.; Christi, M.; et al. Space-based near-infrared CO<sub>2</sub> measurements: Testing the Orbiting Carbon Observatory retrieval algorithm and validation concept using SCIAMACHY observations over Park Falls, Wisconsin. *J. Geophys. Res.* **2006**, *111*, D23303.
27. Connor, B.J.; Boesch, H.; Toon, G.; Sen, B.; Miller, C.; Crisp, D. Orbiting carbon observatory: Inverse method and prospective error analysis. *J. Geophys. Res.* **2008**, *113*, D05305. [[CrossRef](#)]
28. Wunch, D.; Toon, G.C.; Wennberg, P.O.; Wofsy, S.C.; Stephens, B.B.; Fischer, M.L.; Uchino, O.; Abshire, J.B.; Bernath, P.; Biraud, S.C.; et al. Calibration of the total carbon column observing network using aircraft profile data. *Atmos. Meas. Tech.* **2010**, *3*, 1351–1362. [[CrossRef](#)]
29. Wunch, D.; Toon, G.C.; Blavier, J.F.L.; Washenfelder, R.A.; Notholt, J.; Connor, B.J.; Griffith, D.W.T.; Sherlock, V.; Wennberg, P.O. The total carbon column observing network. *Philos. Trans. R. Soc. A* **2011**, *369*, 2087–2112. [[CrossRef](#)] [[PubMed](#)]
30. Schneising, O.; Buchwitz, M.; Reuter, M.; Heymann, J.; Bovensmann, H.; Burrows, J.P. Long-term analysis of carbon dioxide and methane column-averaged mole fractions retrieved from SCIAMACHY. *Atmos. Chem. Phys.* **2011**, *11*, 2863–2880. [[CrossRef](#)]



© 2016 by the authors; licensee MDPI, Basel, Switzerland. This article is an open access article distributed under the terms and conditions of the Creative Commons Attribution (CC-BY) license (<http://creativecommons.org/licenses/by/4.0/>).